Available online at www.sciencedirect.com
SCIENCE DIRECT®
ELSEVIER
Nuclear Instruments and Methods in Physics Research B 228 (2005) 163–169
NIM B
Beam Interactions with Materials & Atoms
www.elsevier.com/locate/nimb

Molecular dynamics simulation of sputtering from a cylindrical track: EAM versus pair potentials

Orenthal J. Tucker [a], Dmitriy S. Ivanov [a], Leonid V. Zhigilei [a,*], Robert E. Johnson [a], Eduardo M. Bringa [b]

[a] *Department of Materials Science and Engineering, University of Virginia, 116 Engineer's Way, Charlottesville, VA 22904-4745, United States*
[b] *Lawrence Livermore National Laboratory, Livermore, CA 94551, United States*

Abstract

Molecular dynamics simulations implementing the thermal spike model for sputtering by energetic particle bombardment are performed for a gold target represented with a many-body embedded atom method (EAM) potential. A linear dependence of sputtering yield on the effective energy deposition is observed over a broad range of sufficiently high excitation energies, suggesting that the conclusions of earlier simulations performed with pair potentials have a general character and are not sensitive to the choice of interatomic potential. At the same time, significant differences in cluster ejection are observed between the simulations performed with EAM and pair potentials. Clusters constitute a much larger fraction of the total yield in the EAM simulations, which is related to the environmental dependence of the interatomic interaction in metals that is correctly reproduced by EAM potential. An apparent disagreement between the analytical thermal spike model and its implementation in MD simulations cannot be attributed to the choice of interatomic potential but reflects a difference in the ejection mechanisms. Thermally activated evaporation from the surface is assumed in the analytical thermal spike model, whereas prompt ejection from a relatively deep part of the excited region and fast non-diffusive cooling of the spike region takes place in MD simulations.

PACS: 61.80; 71.15.D; 79.20.R

1. Introduction

Irradiation of a solid by energetic particles can generate tracks of electronic or collisional excitations and can lead to the ejection (or sputtering) of atoms and clusters from the irradiated surface. This process is relevant to a wide range of

* Corresponding author.
E-mail address: lz2n@virginia.edu (L.V. Zhigilei).

0168-583X/$ - see front matter © 2004 Elsevier B.V. All rights reserved.
doi:10.1016/j.nimb.2004.10.040

phenomena, from sputtering of icy surfaces of the moons of Jupiter [1] to fast ion bombardment under well-controlled laboratory conditions for material characterization [2]. A number of analytical models have been proposed to describe the sputtering process and predict the dependence of the number of ejected particles (sputtering yield Y) on the effective energy deposition (dE/dx) by an incoming projectile. In particular, the thermal spike model has been introduced to describe the sputtering process at high excitation densities, when atomic collisions lead to the formation of an energized cylindrical region in the target. In the thermal spike model a diffusive energy redistribution from the initial energetic cylindrical region is considered and thermally-activated evaporation from the surface is responsible for atomic ejection. Calculations of the sputtering yield, performed within the spike model by integration of the thermal evaporation over time and surface area, predict a roughly quadratic dependence on the deposited energy, $Y \propto (dE/dx)^2$ [3,4]. A large number of laboratory observations for different targets can be relatively well described by this quadratic dependence [5,6]. This was initially thought to support the underlying physical picture.

In order to better constrain free parameters in the thermal spike model, a series of molecular dynamics (MD) simulations were carried out [7–10]. Surprisingly, both the physical processes leading to the material ejection and the dependence of the sputtering yield on the deposited energy appeared to be rather different from that in the conventional thermal spike model. Instead of thermal evaporation from the surface, at high energy densities MD simulations showed an explosive disruption of the excited region, leading to the ejection of both individual atoms and clusters of different sizes. The sputtering yield for the cylindrically energized region of a fixed radius was found to have a steep power-law dependence at small (dE/dx), $Y \propto (dE/dx)^n$ with $n > 2$, and nearly linear dependence at high (dE/dx), $Y \propto (dE/dx)^n$ with $n \approx 1.0$–1.2 [8]. The weaker, as compared to the prediction of the analytical thermal spike model, dependence of the sputtering yield at high (dE/dx) suggests that additional energy dissipation channels are activated in the high-energy regime. It has been suggested based on MD simulations [7] and supported by continuum hydrodynamics calculations [11,12], that the elastic wave driven by the relaxation of the high pressure created within the initial spike can carry away a significant fraction of the deposited energy. Moreover, in the process of thermal and mechanical relaxation of the excited region a significant part of the thermal energy can be transformed to the potential energy of melting, structural changes and cavitation, leading to the fast non-diffusive cooling and lowering the sputtering yield.

A characteristic dependence of the sputtering yield on the excitation energy, with an initial steep increase followed by a linear dependence that holds over a broad range of energies, have been consistently reported in a number of MD simulations performed for model materials of different densities, binding energies and structures [7–10]. In particular, Lennard–Jones (LJ) and Morse interatomic potentials parameterized for Ar, O_2 and Cu have been used in the simulations, and both crystalline and amorphous structures of the target material have been considered. Nevertheless, the question on the applicability of the conclusions obtained in MD simulations to real materials still remains. All the simulations aimed at reproducing the thermal spike conditions have been performed with pair interatomic potentials, mainly LJ. This potential provides a good description of van der Waals interaction in inert gases and molecular systems [13] and is often used, along with other pair potentials, in "generic" MD simulations where the objective is to model a general class of effects and the only requirement is to have a physically reasonable potential with an attractive and a repulsive parts. However, a direct extrapolation of the simulation results to metals, for which most of the laboratory results on sputtering are being reported [5,6,14], is not possible even at a qualitative level.

Although there have been attempts to parameterize LJ [15] and, with somewhat better results, Morse [16] potentials for metals, in general, pair potentials provide a rather poor description of the metallic bonding. The strength of "individual bonds" in metals has a strong dependence on the local environment. It decreases as the local envi-

ronment becomes too crowded due to the Pauli's principle and increases near surfaces and in small clusters due to the localization of the electron density. Pair potentials do not depend on the environment and, as a result, cannot reproduce some of the characteristic properties of metals. In particular, pair potentials significantly, up to 2–3 times, underestimate the ratio between the cohesive energy and the melting temperature of metals and cannot account for a much stronger bonding of atoms near surfaces or in small clusters. Another consequence of the environmental dependence of the interatomic bonding in metals is a significantly lower vapor pressure characteristic of liquid metals as compared to molecular systems or Lennard–Jonesium. Sputtering in the high-energy regime is defined by a complex interplay of thermal evaporation, melting and hydrodynamic motion of the liquid region, ejection of clusters of different sizes, and mechanical relaxation of the material around the thermal spike. Therefore, the inability of pair potentials to correctly describe the melting and evaporation processes, the energy and stability of clusters, as well as the surface energy in metals does not allow one to directly extrapolate the simulation results obtained with pair potentials to metals.

In this paper we report the results of a series of MD simulations of thermal spike sputtering from a Au target performed with a many-body embedded atom method (EAM) interatomic potential [17,18], which provides a computationally efficient yet rather realistic description of the behavior and properties of metals. A brief description of the computational model used in the simulations is given next, in Section 2. The results of the simulations are presented and related to earlier calculations performed with Lennard–Jones and Morse pair potentials in Section 3. A summary on the general and material-specific characteristics of the thermal spike sputtering process is given in Section 4.

2. Computational model

Implementation of the thermal spike model in MD simulations presented in this paper is similar to the one used in earlier works performed with pair potentials [7–10]. The thermal spike is modeled by assigning velocities in random directions to all atoms located within a cylindrical region with radius R_{cyl} located in the center of a rectangular computational cell. The values of the velocities correspond to kinetic energy E_{exc}, which can be related to the effective stopping power of the incident ion, $dE/dx = N_{exc}E_{exc}/d \approx n\pi R_{cyl}^2 E_{exc}$, where N_{exc} is the average number of excited atoms per layer, d is the separation distance between the atomic layers, and n is the number density of the target material. All simulations are performed for R_{cyl} = 10 Å, whereas the excitation energy, E_{exc}, is varied between 2.5 eV and 15 eV. The cohesive energy of the model EAM Au material is $U = 3.93$ eV, and the range of the excitation energies is chosen to include the two regimes that have been identified in earlier simulations [7], the low-energy regime ($E_{exc} \leqslant U$) and the high-energy regime ($E_{exc} > U$).

The initial MD computational cell used in this work is a slab with an FCC crystal structure and periodic boundary conditions applied in the lateral directions, parallel to (1 0 0) free surfaces. Simulations are performed for slabs of two different sizes, $20.4 \times 20.4 \times 16.3$ nm (400,000 atoms) and $16.3 \times 16.3 \times 12.2$ nm (192,000 atoms), with smaller dimension being normal to the free surfaces. No statistically significant difference is observed between the results obtained for the two systems and the results presented in the next section are averages of the two series of simulations. Each simulation of the thermal spike results in the ejections of atoms from the "top" and "bottom" surfaces of the slab. Most of the atoms are ejected from ~1.5 nm deep surface regions of the sample with the maximum depth of origin of an atom ejected in the simulation at the highest excitation energy of 5.5 nm, smaller than a half of the thickness of the smaller slab used in the simulations, 6.1 nm. The ejection processes from the two surfaces of the slab are, therefore, independent from each other and are treated as such in the analysis of the results. Interatomic interaction in the model is described by the embedded-atom method (EAM) with a functional form and parameterization suggested in [18].

3. Results and discussion

A typical snapshot from one of the simulations is shown in Fig. 1(a). Energy deposition within the cylindrical spike region induces a range of processes, including emission and radial propagation of a strong pressure wave, fast melting of the excited region and its immediate surroundings, active hydrodynamic motion near the two surfaces of the computational cell, and the emission of atoms and small clusters from the surfaces. The duration of the simulations is chosen so that all the processes that can contribute to the atomic ejection cease and the ejection yield can be clearly defined.

The dependence of the number of ejected atoms on the excitation energy, is shown in Fig. 2. In order to obtain reliable data for the EAM Au target, each MD simulation for Au is repeated several (2–4) times. Each simulation produces two independent yield values, one from the top surface and another from the bottom surface of the computational cell.

Similarly to the earlier results from MD simulations performed with pair potentials [7–10], we can clearly identify two regimes of atomic ejection, a low-energy regime ($E_{\mathrm{exc}} < U$) with a steep yield dependence on the excitation energy and a high-energy regime ($E_{\mathrm{exc}} > U$) with a weaker, almost linear dependence of the yield. Power-law fit of the data points for Au in the high-energy regime gives $Y \propto (\mathrm{d}E/\mathrm{d}x)^n$ with $n = 1.3 \pm 0.3$. This is in agreement with the results obtained for pair potentials [9], where a similar linear dependence of the yield was observed at $E_{\mathrm{exc}} > U$, with $n = 1.1 \pm 0.2$. Moreover, fitting the yield to the expression suggested in [12], $Y \approx C \times [R_{\mathrm{cyl}}/U] \times [\mathrm{d}E/\mathrm{d}x]$ gives us $C \approx 0.19$ that is very close to the values obtained with pair potentials, $C \approx 0.18$ [12].

The overall good quantitative agreement between the simulation results obtained with EAM and pair potentials is additionally illustrated by plotting in Fig. 2 several data points obtained with LJ pair potential with parameters chosen to represent Ar. Only one simulation was performed with LJ potential for each data point but, despite the statistical uncertainty, a quantitative agreement between the EAM and LJ results is apparent. Note, that in order to make a quantitative compar-

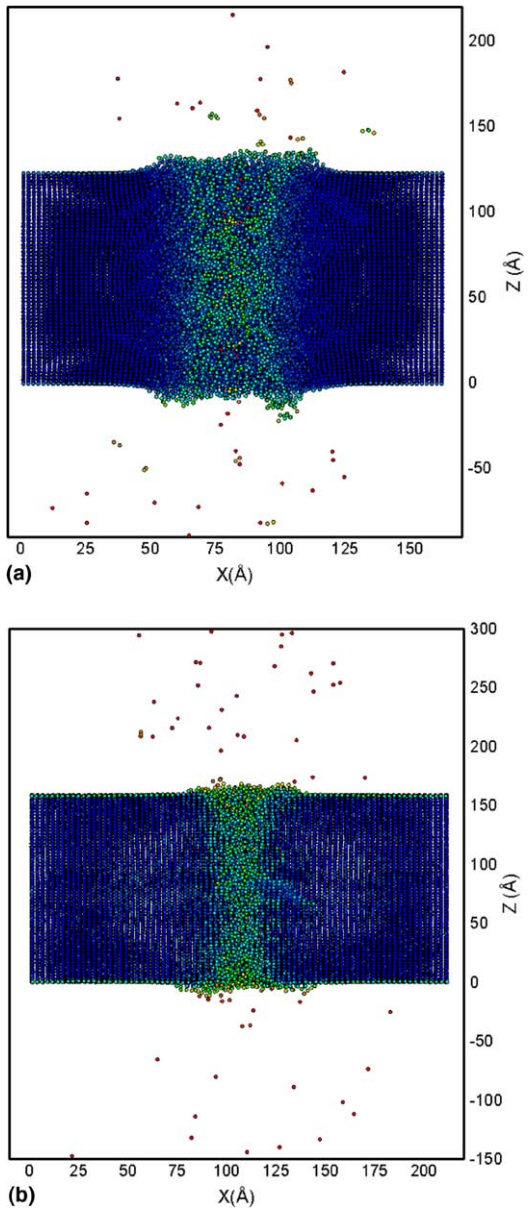

Fig. 1. Snapshots from simulations of thermal spike in Au (a) and Ar (b) performed at the same scaled excitation energy $E_{\mathrm{exc}}/U = 2.56$ and shown for the same scaled time. The real excitation energies and times are $E_{\mathrm{exc}} = 10$ eV and $t = 4$ ps for Au and $E_{\mathrm{exc}} = 0.205$ eV and $t = 15$ ps for Ar. Atoms are colored according to their potential energy, from blue (low energy) to red (high energy). Only half of the computational cell is shown to provide a clear view of the spike region. (For interpretation of the references in color, the reader is referred to the web version of this article.)

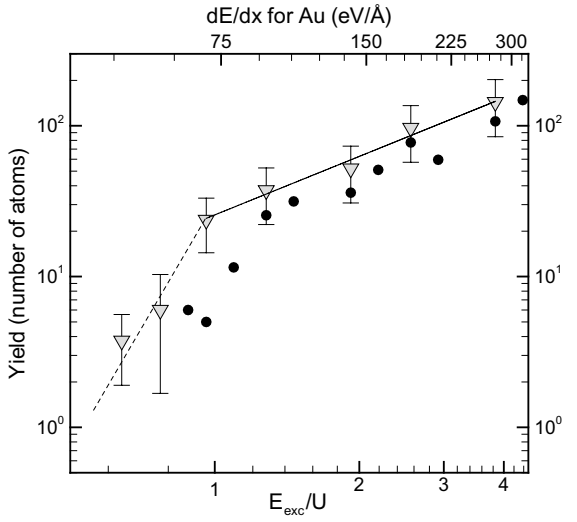

Fig. 2. Yield of ejected atoms obtained in MD simulations of thermal spike of Au (gradients) and Ar (black circles) as a function of the excitation energy. Each point for Au results from the averaging over 4–8 values of the ejection yield with error bars showing the standard error of the mean. The solid line is a power law fit of the data points for Au at excitation energies $E_{exc} > 0.95U$. The dashed line is just a guide to the eye. The data points for Ar correspond to only one simulation performed for each excitation energy.

ison of the simulation results, the size of the computational cell and the radius of the excited region in LJ simulations were scaled by the ratio of the lattice parameters of Au and Ar, $R_{cyl}^{Ar} = R_{cyl}^{Au}(a_{Au}/a_{Ar}) \approx 0.77$, whereas the duration of the LJ simulations was scaled by $t_{Ar} = t_{Au}(U_{Au}/U_{Ar})^{1/2}(M_{Au}/M_{Ar})^{-1/2}(a_{Au}/a_{Ar})^{-1/2} \approx 4.1 \times t_{Au}$, where M_{Au} and M_{Ar} are atomic masses of the two materials.

Although the overall dependence of the sputtering yield appears to be not sensitive to the choice of interatomic potential, we do observe significant differences in the cluster composition of the ejected material between the simulations performed with LJ and EAM potentials. The difference can be noticed in a visual inspection of the snapshots from the simulations. For example, comparison of Figs. 1(a) and (b), where snapshots from the simulations performed for the same scaled excitation energy are shown for the same scaled time, suggests that more clusters are ejected in the Au simulation. This conclusion can be supported by quantitative analysis of cluster contribution to the total yield, Fig. 3. At the same scaled excitation energy, $E_{exc}/U = 1.28$, Figs. 3(a) and (b), contribution of monomers to the total yield is less than 20% for Au and over 40% for Ar. At the same time, dimers account for ~35% and ~12% of the total yield in the Au and Ar simulations respectively. Two largest, 8- and 15-atoms, clusters ejected in the Au simulation, account for more than 33% of the total yield. A similar difference between the two materials is also observed at higher excitation energies. One can see from Figs. 3(c) and (d) that monomers account for approximately 60% of the total yield in the case of Ar and only 38% in the simulation performed for Au.

The tendency for cluster formation in the case of metals represented with EAM potential is not surprising and is a reflection of the dependence of the strength of "individual bonds" on the local environment, which results in a stronger bonding of atoms in small clusters as compared to the bulk, as briefly discussed in Section 1. What is surprising is that the ejection of clusters does not appear to significantly enhance the yield values relative to the simulations performed with pair potentials and has no effect on the overall character of the yield dependence on the excitation energy. The reason for the apparent lack of sensitivity of the total yield to the choice of the interatomic potential may be related to the ejection mechanisms. The atomic ejection appears to be dominated by a prompt ejection from the excited spike region that coincides with the active collective motion of the material and fast non-diffusive cooling of the excited region. We find that almost all of the ejected atoms are coming from the original excited region with ejection depths of ~2.5 nm below the surface. This scenario observed in MD simulations is rather different from the one that would correspond to the thermal evaporation, when most of the atoms would originate from the surface of the target.

4. Summary

We performed MD simulations implementing the thermal spike model with a many-body EAM

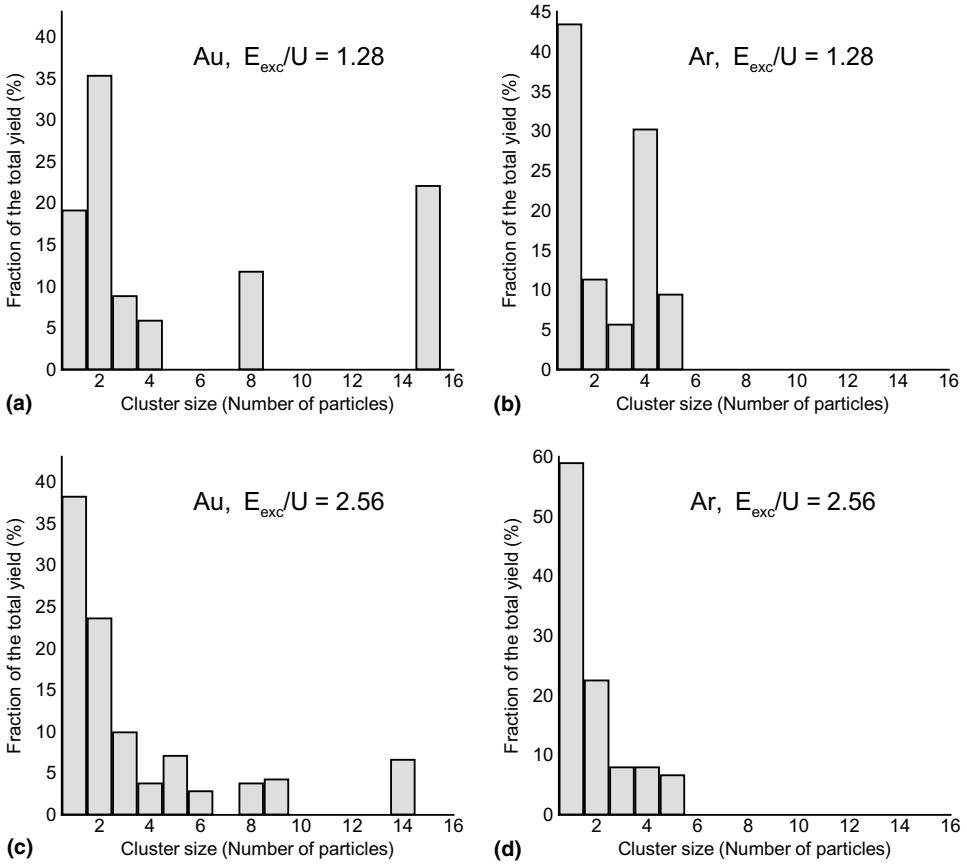

Fig. 3. Contribution of clusters and monomers to the total yield in MD simulations of thermal spike in Au (a,c) and Ar (b,d) performed at two scaled excitation energies $E_{exc}/U = 1.28$ (a,b) and $E_{exc}/U = 2.56$ (c,d).

interatomic potential. For a fixed track radius, the dependence of the total ejection yield observed in the simulations appears to be in a good quantitative agreement with earlier results observed in simulations performed with pair interatomic potentials. Two regimes are identified in the yield dependence on the excitation energy, a low-energy regime with a steep rise of the yield with the energy and a broad high-energy regime with a nearly linear energy dependence of the sputtering yield. The low (dE/dx) regime, in fact, exhibits a dependence similar to that of the thermal spike model [7,8], but the high (dE/dx) regime, which was thought initially to explain a large set of laboratory data [6] does not.

These simulations provide strong support for a nearly linear dependence of the sputtering yield at high (dE/dx) in the MD implementation of a cylindrical spike. This result appears to be not sensitive to the choice of the interatomic potential. At the same time, significant differences in cluster ejection are observed between the simulations performed with EAM and pair potentials. Clusters constitute a much larger fraction of the total yield in the EAM simulations, which may be related to the environmental dependence of the interatomic interaction described by EAM potential. The environmental dependence of interatomic interaction is characteristic for metals and the conclusions of this work on cluster ejection are relevant to sputtering experiments performed for metals. The apparent discrepancy between the analytical thermal spike model and its implementation in MD simulations can not be attributed to the choice of

interatomic potential but is a reflection of a difference in the ejection mechanisms. Thermally activated evaporation from the surface is assumed in the analytical thermal spike model, whereas prompt ejection from a relatively deep part of the excited region and fast non-diffusive cooling of the spike region takes place in MD simulations.

There exists an extensive set of data for incident ions impacting gold [5,19]. These results involve a large range of (dE/dx) in which the effective radius of the excited region also varies. Having confirmed the applicability of the linear sputtering model for this material, we will extend our study to different radii of the excited region and relate simulation results to experimental data in a subsequent paper.

Acknowledgements

Financial support of this work was provided by the Astronomy Division of the National Science Foundation.

References

[1] R.E. Johnson, Rev. Mod. Phys. 68 (1996) 305.
[2] R. Blumenthal, K.P. Caffey, E. Furman, B.J. Garrison, N. Winograd, Phys. Rev. B 44 (1991) 12830.
[3] R.E. Johnson, R. Evatt, Radiat. Eff. Def. Solids 52 (1980) 187.
[4] M. Jakas, Radiat. Eff. Def. Solids 152 (2000) 157.
[5] H.H. Andersen, A. Brunelle, S. Della-Negra, J. Depauw, D. Jacquet, Y. Le Beyec, J. Chaumont, H. Bernas, Phys. Rev. Lett. 80 (1998) 5433.
[6] R.E. Johnson, M. Pospieszalska, W.L. Brown, Phys. Rev. B 44 (1991) 7263.
[7] E.M. Bringa, R.E. Johnson, M. Jakas, Phys. Rev. B 60 (1999) 15107.
[8] E.M. Bringa, R.E. Johnson, Nucl. Instr. and Meth. B 143 (1998) 513.
[9] E.M. Bringa, R.E. Johnson, L. Dutkiewicz, Nucl. Instr. and Meth. B 152 (1999) 267.
[10] H.M. Urbassek, H. Kafemann, R.E. Johnson, Phys. Rev. B 49 (1994) 786.
[11] M.M. Jakas, E.M. Bringa, Phys. Rev. B 62 (2000) 824.
[12] M.M. Jakas, E.M. Bringa, R.E. Johnson, Phys. Rev. B 65 (2002) 165425.
[13] D.V. Matyushov, R. Schmid, J. Chem. Phys. 104 (1996) 8627.
[14] H.H. Andersen, A. Johansen, V.S. Touboltsev, Nucl. Instr. and Meth. B 164–165 (2000) 727.
[15] T. Halicioğlu, G.M. Pound, Phys. Stat. Sol. 30 (1975) 619.
[16] L.A. Girifalco, V.G. Weizer, Phys. Rev. 114 (1959) 687.
[17] M.S. Daw, S.M. Foiles, M.I. Baskes, Math. Sci. Rep. 9 (1993) 251.
[18] X.W. Zhou, H.N.G. Wadley, R.A. Johnson, D.J. Larson, N. Tabat, A. Cerezo, A.K. Petford-Long, G.D.W. Smith, P.H. Clifton, R.L. Martens, T.F. Kelly, Acta Mater. 49 (2001) 4005.
[19] A. Brunelle, S. Della-Negra, J. Depauw, D. Jacquet, Y. Le Beyec, M. Pautrat, K. Baudin, H.H. Andersen, Phys. Rev. A 63 (2001) 022902.